Scanned–Array Audio Beamforming using 2^{nd}– and 3^{rd}–Order 2D IIR Beam Filters on FPGA

N. Ganganath*, G. Attanayake*, T.Y. Bandara*, P. Ilangakoon*, R. Rodrigo*, A. Madanayake† and L.T. Bruton‡
*Department of Electronic and Telecommunication Engineering, University of Moratuwa, Moratuwa 10400, Sri Lanka
†Electrical and Computer Engineering University of Akron, Akron, OH, USA 44325-3904
‡Department of Electrical and Computer Engineering, University of Calgary, Calgary, Alberta T2N 1N4, Canada
Email: arjuna@uakron.edu ranga@ent.mrt.ac.lk

***Abstract*—Real-time scanned-array direct-form-I hardware implementations of two-dimensional (2D) infinite impulse response (IIR) frequency-planar beam plane-wave (PW) filters have potentially wide applications in the directional enhancement of spatio-temporal broadband PWs based on their directions of arrival (DOAs). The proposed prototypes consist of a microphone sensor array, low-noise-amplifiers (LNAs), multiplexers (MUXs), a programmable gain amplifier (PGA), an analog to digital converter (ADC), a digital to analog converter (DAC), and a field programmable gate array (FPGA) circuit based 2D IIR spatio-temporal beam filter implemented on a single Xilinx Virtex2P xc2vp30-7ff896 FPGA chip. Starting from published 1^{st}-order designs, novel FPGA architectures for highly-selective 2^{nd}- and 3^{rd}-order beam PW filters are proposed, simulated, implemented on FPGA, and verified on-chip.**

***Index Terms*—2D, audio, beamforming, FPGA.**

I. INTRODUCTION

Multi-dimensional (MD) beam filters facilitate the selective filtering of spatio-temporal broadband PWs based on their DOA [1]. Real-time audio signal processing using linear microphone arrays have many applications such as sound localization [2] and directional audio systems [3]. Passive inductor-resistor (LR) networks are used to realize 2D infinite impulse response (IIR) recursive filters [1]. Multi-dimensional IIR frequency-planar PW filters obtained from resistively-terminated passive inductor-capacitor (LC) prototypes are practical bounded-input-bounded-output (BIBO) stable [4] and are of low computational complexity [1].

We propose a scanned-array audio beamformer using highly selective 2^{nd}- and 3^{rd}-order 2D IIR frequency-planar beam filters. The proposed architecture employs scanned-array data acquisition [5] to achieve low hardware complexity, and on-chip data acquisition at each of the element in the uniform linear array (ULA) of sensors.

II. REVIEW OF FREQUENCY-PLANAR BEAM FILTERS

The 2D space-time input signal is of the form [6]

$$w(n_1,n_2) = w_{pass}(l_0) + \sum_{k=1}^{M} w_{stop}(l_k) + n_v(n_1,n_2) \quad (1)$$

where $l_k = -\sin\theta_k n_1 \Delta x + n_2 c\Delta T_s$, $0 \le n_2$ and $0 \le n_1 < N_1$ corresponds to the linear array of N_1 sensors which are

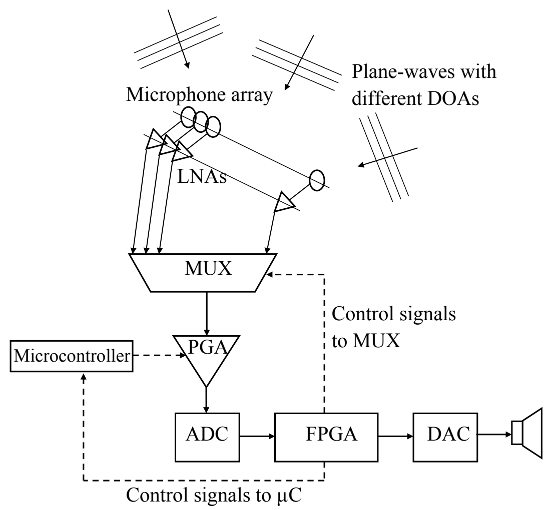

Fig. 1. Complete system architecture.

uniformly space Δx apart and sampled at each ΔT_s seconds.The speed of wave propagation is c. Thus $\theta_k | 0 \le k \le M$ are the possible spatial DOAs. $w_{pass}(l_0)$ is the pass-band signal to be enhanced whereas $w_{stop}(l_k)$, $k = 1, 2, \ldots, M$ are the undesired PWs to be attenuated. Term $n_v(n_1, n_2)$ represents the non-plane wave sampled signals such as broadband noise and interference. Fig. 2(a) and (b) illustrate the mapping between space-space DOA $\theta (0 \le \theta \le 90^0)$ and space-time DOA $\psi(0 \le \psi \le 45^0)$ which is given by [7],

$$\psi_k = \tan^{-1}\left(\frac{\Delta x \sin\theta_k}{c\Delta T_s}\right) \quad (2)$$

2D Nyquist condition should be satisfied in order to avoid 2D aliasing, and then $\Delta x = c\Delta T_s$ resulting $\tan\psi_k = \sin\theta_k$ [6]. Frequency-planar beam filters are capable of highly-selective directional enhancement of broadband spatio-temporal plane waves based on their DOA. Consider the 2D Fourier transform pair $w_{pass}(\Delta x n_1, c\Delta T_s n_2, \psi) \overset{2D}{\Leftrightarrow} W_{pass}(j\omega_1, j\omega_2, \psi)$ for the pass-band 2D spatio-temporal PW signal $w_{pass}(-\sin\theta_0 n_1 \Delta x + n_2 c\Delta T_s)$. If the 2D Nyquist condition is satisfied, the normalized region of support (ROS) of $W_{pass}(j\omega_1, j\omega_2, \psi)$ within the Nyquist square $(-\pi < \omega_1 < \pi, -\pi < \omega_2 < \pi)$ closely surrounds a straight line. As illustrated in Fig 2(c), this ROS passes through the origin

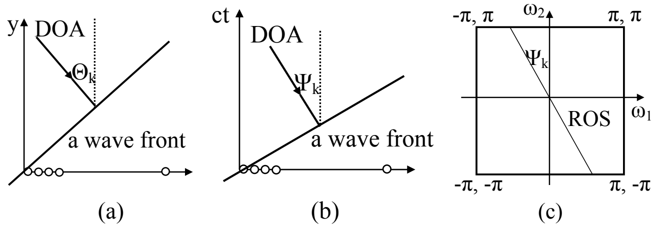

Fig. 2. (a) Incident plane-wave in space, (b) incident plane-wave in space-time and, (c) its frequency-domain ROS within the 2D Nyquist square.

in $(\omega_1, \omega_2) \in R^2$, inclining at an angle ψ to the ω_2 axis. The principle of spectral beam filtering of broadband PWs requires the 2D beam-shaped passband to closely surround the ROS of $W_{pass}(j\omega_1, j\omega_2, \psi)$ for selectively filtering the sampled plane wave while rejecting the stop band spectrum $w_{stop}(\Delta x n_1, c\Delta T_s n_2, \psi) \overset{2D}{\Leftrightarrow} W_{stop}(j\omega_1, j\omega_2, \psi)$ [1].

III. Synthesis of 2D IIR Beam Filters using Network Resonance

A highly-selective computationally efficient practical-BIBO stable implementation of a 2D IIR frequency planar beam PW digital filter can be designed using the concept of network resonance [1]. Synthesis of 1^{st}-order 2D IIR beam filter is described in [6].

A. Second-Order 2D IIR Frequency-Planar Beam Filter

We propose the 2^{nd}-order implementation of a 2D IIR frequency-planar beam PW digital filter design starting from the 2^{nd}-order resistively terminated passive prototype 2D network illustrated in Fig.4(a). Such networks have an s-domain transfer function given by [1],

$$T(s) = \frac{Y(s)}{W(s)} = \frac{R_L}{R_s + R_L + (L_1 + C_2 R_s R_L)s + C_2 R_L L_1 s^2} \tag{3}$$

By applying frequency-planar transformation, $s = s_1 \cos\psi + s_2 \sin\psi$ and taking $L_i = L_1 \cos\psi$, $L_j = L_2 \sin\psi$, $C_i = C_2 \cos\psi$, $C_j = C_2 \sin\psi$, $R_L = 1$, we get

$$T(s_1, s_2) = \frac{1}{[e_1 + e_2 s_1 + e_3 s_2 + e_4 s_1^2 + e_5 s_2^2 + e_6 s_1 s_2]} \tag{4}$$

where $e_1 = 1 + R_s$, $e_2 = L_i + R_s C_i$, $e_3 = L_j + R_s C_j$, $e_4 = L_i C_i$, $e_5 = L_j C_j$ and $e_6 = L_i C_j + L_j C_i$. We can obtain the values of L_1, L_3, C_2 and R_s using [8] (pp.312). By discretizing (4) using the 2D bilinear transformation,

$$s_k = \frac{1 - z_k^{-1}}{1 + z_k^{-1}}, k = 1, 2 \tag{5}$$

we get the **z**-domain transfer function [1],

$$H(z_1, z_2) = T(s_1, s_2)\big|_{s_1 = \frac{1-z_1^{-1}}{1+z_1^{-1}}, s_2 = \frac{1-z_2^{-1}}{1+z_2^{-1}}} \tag{6}$$

Applying inverse double **z**-transform to the (6) yields the time domain difference equation [1],

$$y(n_1, n_2) = \sum_{i=0}^{2}\sum_{j=0}^{2} a_{ij} w(n_1 - i, n_2 - j) - \sum_{i=0}^{2}\sum_{j=0}^{2} b_{ij} y(n_1 - i, n_2 - j) \tag{7}$$

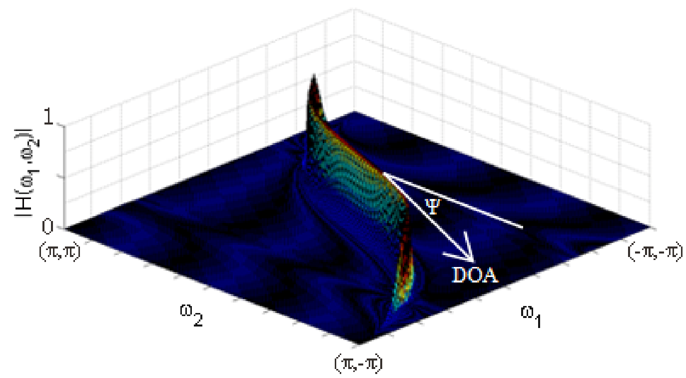

Fig. 3. Magnitude transfer function of 2D IIR frequency-planer beam filter.

For the feed-back path $i + j \neq 0$ where $0 \le n_1 < N_1$ and $0 \le n_2$. The feed-forward coefficients $a_{ij} = 1$ for $i, j = 1, 2$ and feed-back coefficients are given by,

$$\begin{aligned}
b_{10} &= (2e_1 + 2e_3 - 2e_4 + 2e_5)/A \\
b_{01} &= (2e_1 + 2e_2 + 2e_4 - 2e_5)/A \\
b_{11} &= (4e_1 - 4e_4 - 4e_5)/A \\
b_{20} &= (e_1 - e_2 + e_3 + e_4 + e_5 - e_6)/A \\
b_{02} &= (e_1 + e_2 - e_3 + e_4 + e_5 - e_6)/A \\
b_{12} &= (2e_1 - 2e_3 - 2e_4 + 2e_5)/A \\
b_{21} &= (2e_1 - 2e_2 + 2e_4 - 2e_5)/A \\
b_{22} &= (e_1 - e_2 - e_3 + e_4 + e_5 + e_6)/A
\end{aligned} \tag{8}$$

where $A = e_1 + e_2 + e_3 + e_4 + e_5 + e_6$. The ZICs are given by,

$$w(-i, n_2) \equiv y(-i, n_2) \equiv 0 \; and \; w(n_1, -i) \equiv y(n_1, -i) \equiv 0 \tag{9}$$

where $i = 1, 2$.

B. Third-Order 2D IIR Frequency-Planar Beam Filter

Similar to the 2^{nd}-order case, 2D Laplace transfer function of the LRC network illustrated in Fig.4(b) is given by,

$$\begin{aligned} T(s) = \frac{Y(s)}{W(s)} &= R_L/[R_S + R_L + (L_1 + L_3 + C_2 R_S R_L)s \\ &+ (C_2 L_3 R_S + C_2 R_L L_1)s^2 + C_2 L_1 L_3 s^3)] \end{aligned} \tag{10}$$

By applying frequency-planar transformation and taking $L_i = L_1 \cos\psi$, $L_j = L_1 \sin\psi$, $L_k = L_3 \cos\psi$, $L_l = L_3 \sin\psi$, $C_i = C_2 \cos\psi$, $C_j = C_2 \sin\psi$, $R_L = 1$ we get,

$$\begin{aligned} T(s_1, s_2) = 1/[&e_1 + e_2 s_1 + e_3 s_2 + e_4 s_1^2 + e_5 s_2^2 + e_6 s_1 s_2 \\ &+ e_7 s_1^3 + e_8 s_2^3 + e_9 s_1^2 s_2 + e_{10} s_1 s_2^2] \end{aligned} \tag{11}$$

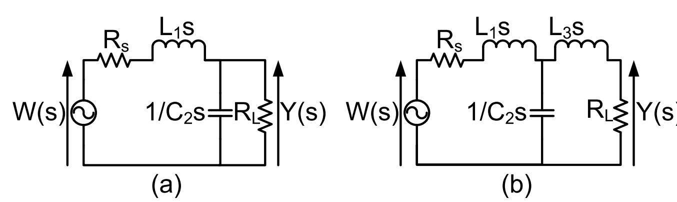

Fig. 4. (a) 2D passive LRC frequency-planar beam network for 2^{nd}-order, (b) 2D passive LRC frequency-planar beam network for 3^{rd}-order.

where $e_1 = 1+R_S$, $e_2 = L_i+L_k+R_SC_i$, $e_3 = L_j+L_l+R_SC_j$, $e_4 = L_iC_i + L_kC_i$, $e_5 = L_jC_j + L_lC_j$, $e_6 = L_iC_j + L_jC_i + L_kC_j + L_lC_i$, $e_7 = L_iL_kC_i$, $e_8 = L_jL_lC_j$, $e_9 = L_iL_kC_j + L_iL_lC_i + L_jL_kC_i$ and $e_{10} = L_iC_iL_l + L_jL_kC_j + C_iL_jL_l$. We can obtain the values of L_1, L_3, C_2 and R_S using [8] (pp.312). By discretizing (11) using the 2D bilinear transformation and applying inverse double $\mathbf{z}$-transform yields the time-domain difference-equation [1],

$$y(n_1,n_2) = \sum_{i=0}^{3}\sum_{j=0}^{3} a_{ij}w(n_1-i,n_2-j) - \sum_{i=0}^{3}\sum_{j=0}^{3} b_{ij}y(n_1-i,n_2-j) \quad (12)$$

For the feed-back path $i+j \neq 0$ where $0 \leq n_1 < N_1$ and $0 \leq n_2$. The feed-forward coefficients $a_{ij} = 1$ for $i,j = 1,2,3$ and feed-back coefficients are given by,

$$\begin{aligned}
b_{10} &= (3e_1 + e_2 + 3e_3 - e_4 + 3e_5 + e_6 - 3e_7 + 3e_8 - e_9 + e_{10})/A\\
b_{01} &= (3e_1 + 3e_2 + e_3 + 3e_4 - e_5 + e_6 + 3e_7 - 3e_8 + e_9 - e_{10})/A\\
b_{11} &= (9e_1 + 3e_2 + 3e_3 - 3e_4 - 3e_5 + e_6 - 9e_7 - 9e_8 - e_9 - e_{10})/A\\
b_{20} &= (3e_1 - e_2 + 3e_3 - e_4 + 3e_5 - e_6 + 3e_7 + 3e_8 - e_9 - e_{10})/A\\
b_{02} &= (3e_1 + 3e_2 - e_3 + 3e_4 - e_5 - e_6 + 3e_7 + 3e_8 - e_9 - e_{10})/A\\
b_{21} &= (9e_1 - 3e_2 + 3e_3 - 3e_4 - 3e_5 - e_6 + 9e_7 - 9e_8 - e_9 + e_{10})/A\\
b_{12} &= (9e_1 + 3e_2 - 3e_3 - 3e_4 - 3e_5 - e_6 - 9e_7 + 9e_8 + e_9 - e_{10})/A\\
b_{22} &= (9e_1 - 3e_2 - 3e_3 - 3e_4 - 3e_5 + e_6 + 9e_7 + 9e_8 + e_9 + e_{10})/A\\
b_{30} &= (e_1 - e_2 + e_3 + e_4 + e_5 - e_6 - e_7 + e_8 + e_9 - e_{10})/A\\
b_{03} &= (e_1 + e_2 - e_3 + e_4 + e_5 - e_6 + e_7 - e_8 - e_9 + e_{10})/A\\
b_{31} &= (3e_1 - 3e_2 + e_3 + 3e_4 - e_5 - e_6 - 3e_7 - 3e_8 + e_9 + e_{10})/A\\
b_{13} &= (3e_1 + e_2 - 3e_3 - e_4 + 3e_5 - e_6 - 3e_7 - 3e_8 + e_9 + e_{10})/A\\
b_{32} &= (3e_1 - 3e_2 - e_3 + 3e_4 - e_5 + e_6 - 3e_7 + 3e_8 - e_9 + e_{10})/A\\
b_{23} &= (3e_1 - e_2 - 3e_3 - e_4 + 3e_5 + e_6 + 3e_7 - 3e_8 + e_9 - e_{10})/A\\
b_{33} &= (e_1 - e_2 - e_3 + e_4 + e_5 + e_6 - e_7 - e_8 - e_9 - e_{10})/A
\end{aligned} \quad (13)$$

where $A = e_1 + e_2 + e_3 + e_4 + e_5 + e_6 + e_7 + e_8 + e_9 + e_{10}$. The ZICs are given by,

$$w(-i,n_2) \equiv y(-i,n_2) \equiv 0 \; and \; w(n_1,-i) \equiv y(n_1,-i) \equiv 0 \quad (14)$$

where $i = 1,2,3$.

IV. FPGA-Architectures for 2^{nd}– and 3^{rd}–Order 2D IIR Beam Plane-Wave Filters

The input is obtained using a $N_1:1$ analog MUX bank and an ADC as shown in Fig.1. The MUXs are switched using a control signal from FPGA and each MUX has a digital input selection port that is used to generate the multiplexed asynchronously sampled scanned-array 1D input signal $w_{scan}(k\triangle T_{as})$ [5]. For the brevity, T_{as} is normalized to 1, hence yielding the expression $w_{scan}(k)$. This signal is fed into the proposed 2^{nd}- and 3^{rd}-order 2D IIR beam filters implemented on a single $Xilinx\ Virtex2P\ xc2vp30-7ff896$ FPGA chip resulting the output $y_{scan}(k)$. Hardware mapped signal flow graphs (SFGs) of scanned-array filter architectures are illustrated in Fig. 5. Spatial Delay Processors (SDPs) in the SFG handle ZICs by connecting a register-stored 0 value to its output when ZICs are required and allow the direct connection from its input to the output otherwise.

The proposed 3^{rd}-order filter consumed 2638 slices out of 13696 and 36 18×18 multipliers out of 136. The critical path delay was $T_{CLK} = 26.527$ns at 422 logic levels. The complete

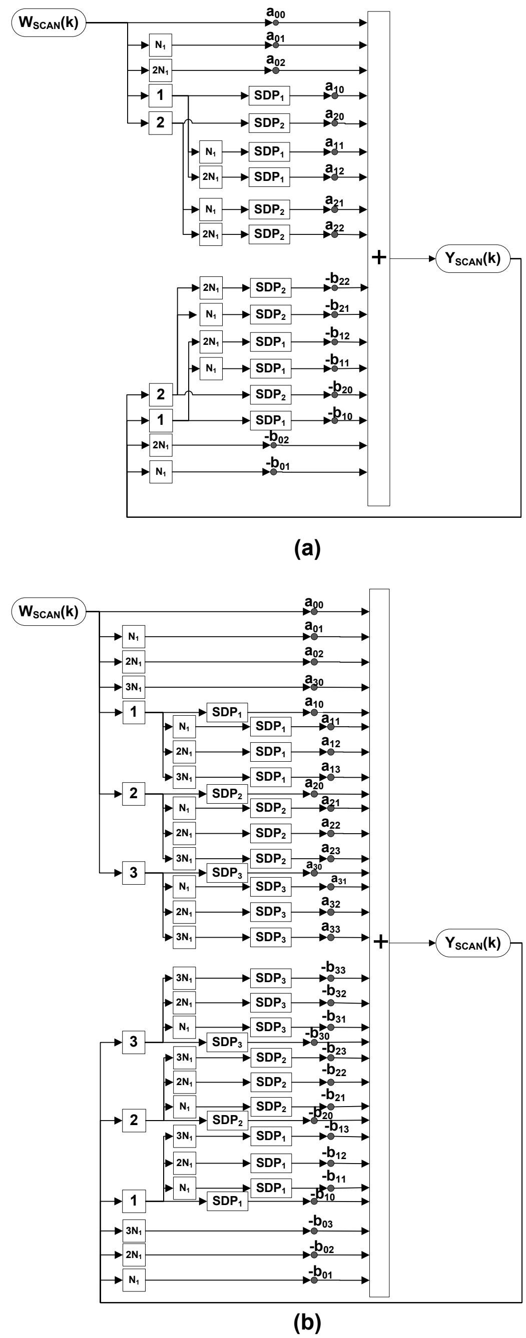

Fig. 5. Hardware mapped SFG of a scanned-array (a) 2^{nd}-order 2D filter architecture (b) 3^{rd}-order 2D filter architecture

system is clocked at 1MHz, which was derived from 100MHz system clock by using Xilinx digital clock manager (DCM) and VHDL clock divider modules.

V. Results

We demonstrate the capability of the 2D IIR beam filters using broad-band Gaussian-pulse PW signals [6]. The pass-band signal has spatial DOA $\theta_0 = 10^0$ and arbitrary selected

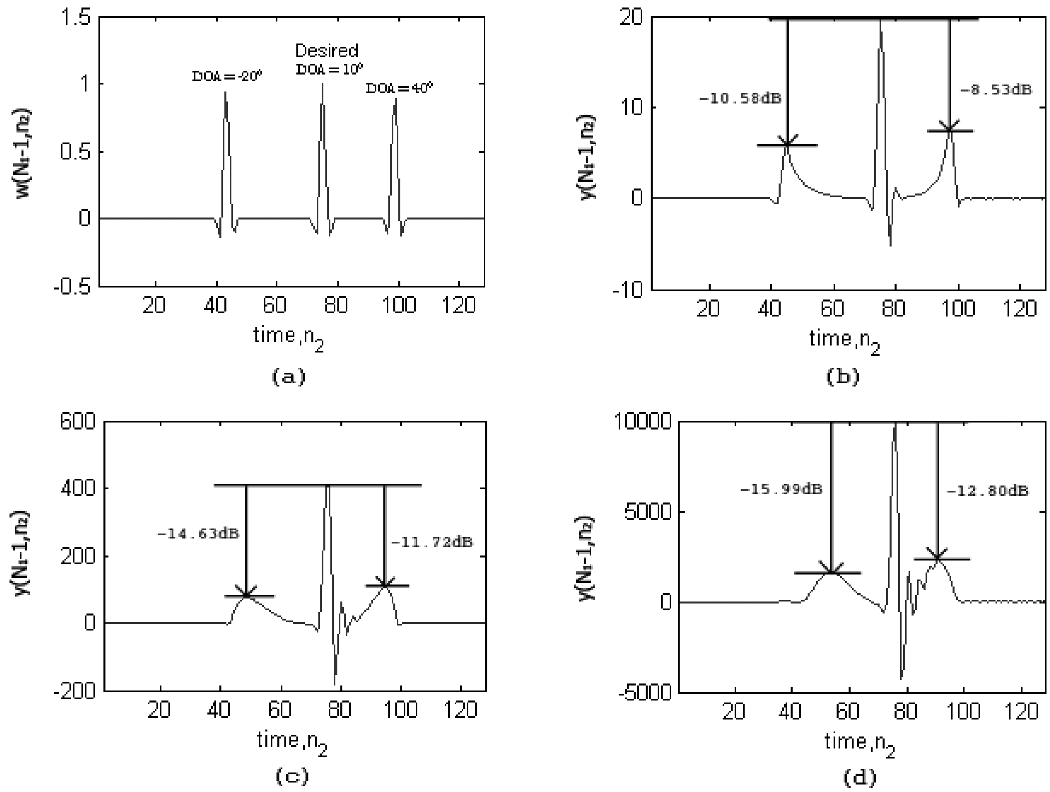

Fig. 6. (a) Input signal sampled by the sensor at $n_1 = 63 (N_1 = 63)$, (b) Output 1D signal of the first-order IIR 2D beam filter $(N_1 = 63)$, (c) Output 1D signal of the 2^{nd}-order IIR 2D beam filter $(N_1 = 63)$, (d) Output 1D signal of the 3^{rd}-order IIR 2D beam filter $(N_1 = 63)$.

two stop-band signals have spatial DOAs $\theta_1 = 40^0$ and $\theta_2 = -20^0$. The objective is to employ a 1^{st}-, 2^{nd}-, and 3^{rd}-order spatio-temporal 2D IIR broadband frequency-planar beam filters to selectively enhance the pass-band PW while attenuating the stop-band waves. Fig 6(a) shows the sampled version of the 2D input signal at $n_1 = 63$ where the total number of microphones is equal to 64. As seen from Fig. 6(b-d), it is clear that the selectivity of the 2D IIR beam filter increases with increased transfer-function order, for a given number of sensors.

VI. Conclusion

Highly selective 2D IIR PW beam-filters are capable of scanned-array audio beamforming. The order of the 2D IIR filters has a substantial effect on the selectivity such that higher the order of the beam filters, higher the selectivity. Real-time audio beamforming applications require sensor array with higher number of sensors in order to obtain a better spatial selectivity. Further scanned-array approach reduces the hardware complexity that is arisen due to the increment of number of channels. Proposed scanned-array audio beam forming architecture can be used in highly selective, low cost and low complexity real-time applications. Novel FPGA hardware architectures for 2^{nd}- and 3^{rd}-order scanned-array frequency-planar beam space-time PW filters were proposed, designed, simulated, physically implemented and finally verified on a single FPGA chip.

Acknowledgment

Authors thank N.M.K Group of Companies, Sri Lanka, University of Akron, USA, and NSERC, Canada for the financial support.

References

[1] L. T. Bruton and N. R. Bartley, "Three-Dimensional Image Processing Using the Concept of Network Resonance," vol. 32. IEEE Transactions on Circuits and Systems, July 1985, pp. 664–672.

[2] J. L. Flanagan, H. F. Silverman, W. R. Patterson, and D. Rabinkin, "A Digital Processing System for Source Location and Sound Capture by Large Microphone Arrays." Proc. IEEE Int. Conf. Acoust., Speech, Signal Process. (ISCASSP97), 1997, pp. 251–254.

[3] E. Weinstein, K. Steele, A. Agarwal, and J. Glass, "LOUD: A 1020-Node Microphone Array and Acoustic Beamformer." Cairns, Australia: International Congress on Sound and Vibration (ICSV), July 2007.

[4] P. Agathoklis and L. T. Bruton, "Practical-BIBO Stability of N-Dimensional Discrete Systems," vol. 130, pt. G, no. 6. Proc. IEE., December 1983, pp. 236–242.

[5] A. Madanayake and L. Bruton, "On The Design and FPGA Implementation of Real-time Scanned-array 2D Frequency-planar Beam Filters." Vienna, Austria: European Association for Signal Processing, EUSIPCO2004, September 2004, pp. 2011–2014.

[6] A. Madanayake and L. T. Bruton, "Low-complexity distributed parallel processor for 2D IIR broadband beam plane-wave filters," *Canadian Journal of Electrical and Computer Engineering (CJECE)*, vol. 32, no. 3, pp. 123–131, Summer 2007.

[7] D. E. Dudgeon and R. M. Mersereau, *Multidimensional Digital Signal Processing*. Englewood Cliffs, N.J. 07632, 1984.

[8] A. I. Zverev, *Handbook of Filter Synthesis*, 1st ed. Wiley-Interscience, January 1967.